Stability of Pattern Formation in Systems with Dynamic Source Regions

M. Majka,* R. D. J. G. Ho,† and M. Zagorski‡
Institute of Theoretical Physics and Mark Kac Center for Complex Systems Research, Jagiellonian University, Łojasiewicza 11, 30-348 Kraków, Poland

(Received 29 June 2022; accepted 27 January 2023; published 1 March 2023)

We explain the principles of gene expression pattern stabilization in systems of interacting, diffusible morphogens, with dynamically established source regions. Using a reaction-diffusion model with a step-function production term, we identify the phase transition between low-precision indeterminate patterning and the phase in which a traveling, well-defined contact zone between two domains is formed. Our model analytically explains single- and two-gene domain dynamics and provides pattern stability conditions for all possible two-gene regulatory network motifs.

DOI: 10.1103/PhysRevLett.130.098402

Reaction-diffusion dynamics with threshold-enhanced production is encountered in many branches of physics, such as the study of combustion [1], neural signaling [2–4], climate evolution [5,6], population dynamics [7–11], chemical reactions, and phase coexistence [12,13]. Reaction diffusion dynamics is also the basic process that governs the spreading of morphogens across a developing tissue [14–19]. Target genes interpret morphogen signals to form gene expression patterns (GEPs). Many aspects of the patterning process have already been investigated, including the scaling of GEPs as an embryo grows [20–26], the precision of domain boundary localization in emerging patterns [27–36], and the relations between structure and function of gene regulatory networks (GRNs) that drive pattern formation [37–47]. However, some important problems remain unaddressed. In particular, little is known about systems where diffusible gene products affect the size of their own source regions (domains). Such dynamic source regions could expand or shrink in unbounded manner, yet, these scenarios are mitigated by additional regulatory mechanisms. This is encountered in spinal cord development [48–50], limb formation [26,51–53], and *Drosophila* wing and eye development [54–56]. In this Letter we elucidate the general physical principles behind the GEP stabilization for one and two genes as well as any combination of regulatory interactions in the system. While we use the language of genes, our analysis is not limited to biological context.

We focus our analysis on the contact zone between two gene expression domains, situated at the opposite sides of a system. The contact zone is either a gap between the domains or their partial overlap [see Figs. 1(a)–1(g)]. The gap corresponds to the stripe of undifferentiated cells. The overlap can be interpreted in two ways: either as the tissue co-expressing two specific target genes [57] or as the imprecise boundary region between domains, where the actual cells in the developing tissue would commit to one of the two fates [27,29]. First, we provide exact classification of domain dynamics for one gene. Then, for two-gene systems, we characterize the phase transition between the phase with unbounded expansion of the overlap, leading to the *indeterminate* GEP [IGEP, Fig. 1(a)] and the phase of *traveling* GEP (TGEP). In the latter case, a stable, fixed-size contact zone is formed, though it can still travel as one entity, as the domains change size in a coordinated manner [Figs. 1(b) and 1(c)]. The transition is controlled by the strength of gene-gene regulatory interactions. Among TGEPs, nonmoving *stable* GEPs (SGEPs) are identified, for which the drift velocity of contact zone is exactly zero [Figs. 1(d) and 1(e)]. We identify the exact relations between system parameters that ensure the formation of SGEPs. Our results are mostly analytical, supported by numerics where necessary.

In the biological context, SGEP might be difficult to achieve as it requires specific combinations of system parameters. However, systems that can be mapped into the vicinity of SGEP in parameter space are guaranteed to form low-velocity TGEPs. Drifting GEPs were observed in *Drosophila* (shifting of posterior gap gene domains) [46,47], in spinal cord development [24,27,58] and limb formation [51,52]. As development happens on finite timescales, slowly moving TGEPs and SGEPs might be similarly efficient in their biological role and both might be practically indistinguishable in experiments.

A convenient model for investigating the GEP stability was first introduced to study the four-gene domain size regulation mechanism in *Drosophila* [59] and the stability of a single traveling domain subjected to extrinsic perturbations and intrinsic noise [60]. The model included a reaction-diffusion equation with a step-function production term. The approximation of interacting kinks, representing the domain boundaries, was utilized in both works to obtain the results. Here, we employ a similar model as in [59,60], but instead of using a moving kink approximation, we

 © 2023 American Physical Society

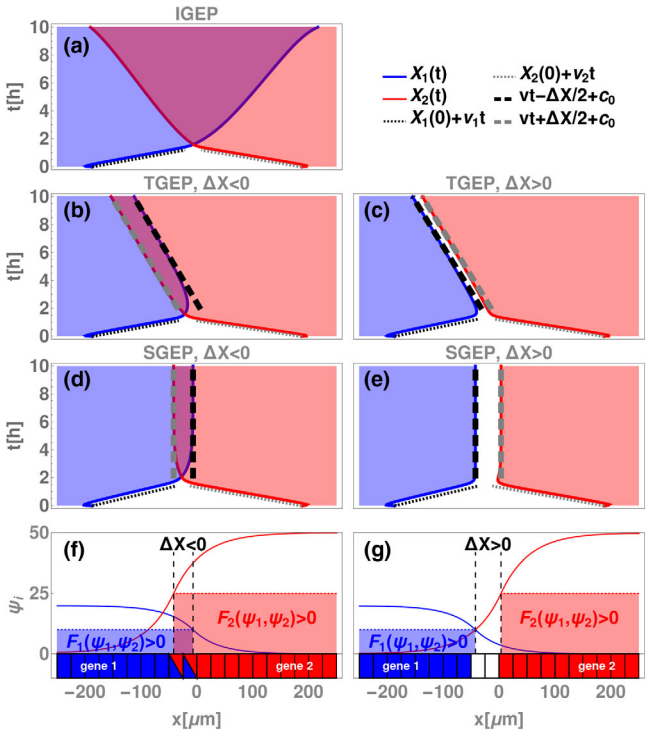

FIG. 1. Exemplary dynamics of GEPs generated by Eq. (1), for self-activating ($\epsilon_{ii} > 0$) and cross-repressive ($\epsilon_{i\neq j} < 0$) gene interactions. Other parameters are chosen in the biologically relevant range (see SM). Red and blue shading indicate domains of active morphogen production, the positions of domain boundaries are found numerically [$X_i(t)$, red and blue solid line] and analytically (gray and black lines). (a) IGEP, unbounded expansion of overlap. (b),(c) TGEP, fronts move to the left, for $t \lesssim 2$ h (dotted lines) front velocities v_i are found from Eq. (10). For $t \gtrsim 4$ h (dashed lines) common velocity v and width ΔX are found from Eq. (11). c_0 is determined numerically to match the analytical and numerical results. (d),(e) SGEP, $v = 0$, parameters satisfy stability conditions (14). Contact zone is an overlap [(b), (d)] or a gap [(c), (e)]. (f),(g) relation between morphogen concentration profiles, GEP, and cellular interpretation of GEP.

identify the conservation law, which allows for exact analytical treatment.

In this Letter we will relate the diffusible gene products with morphogens and the gene expression domains with morphogen source regions. We consider two morphogens that undergo diffusion and degradation and are able to affect each other and their own production. The space-time concentration profile $\psi_i(x,t)$ (ψ_i, for brevity) of each morphogen obeys the equation

$$\partial_t \psi_i = D_i \partial_{xx} \psi_i - \gamma_i \psi_i + H_i \theta(F_i(\psi_1, \psi_2)) \qquad (1)$$

where we have diffusion constant D_i, degradation rate γ_i, production rate in activated state H_i, and Heaviside step function $\theta(\cdots)$. Gene expression is often characterized by Hill-type kinetics with steep increase near the activation threshold [33,61,62], for which the Heaviside function is a generic approximation. The functions $F_i(\psi_1, \psi_2)$ are the activation conditions corresponding to the two-gene motif of the GRN. In linear approximation

$$F_i(\psi_1, \psi_2) \simeq \epsilon_{ii}\psi_i + \epsilon_{ij}\psi_j - C_i. \qquad (2)$$

Here ϵ_{ij} are the interaction coefficients, $\epsilon_{ij} > 0$ indicates activation, and $\epsilon_{ij} < 0$ the inhibition of production. C_i is the threshold for production, possibly affected by the external influence of the GRN on the ith node. Thus, we consider both $C_i > 0$ (gene requires activation) and $C_i < 0$ (gene is active by default).

The regions where $F_i(\psi_1, \psi_2) > 0$ are identified as expression domains and constitute the GEP. The relation between morphogen concentration ψ_i and underlying GEP is illustrated in Figs. 1(f) and 1(g).

Four effective parameters characterize the system:

$$\lambda_i = \sqrt{\frac{D_i}{\gamma_i}}, \quad \tilde{\psi}_i = \frac{H_i}{\gamma_i}, \quad S_i = \frac{2C_i}{\epsilon_{ii}\tilde{\psi}_i}, \quad \chi_i = \frac{\epsilon_{ij}\tilde{\psi}_j}{\epsilon_{ii}\tilde{\psi}_i}. \qquad (3)$$

λ_i is the effective distance traveled by morphogen particle before degradation and it quantifies the range of interactions. $\tilde{\psi}_i$ is the equilibrium concentration level to which the ith morphogen tends in the absence of cross-interactions ($\epsilon_{i\neq j} = 0$) and diffusion. S_i is the effective activation threshold and χ_i describes the relative strength of cross- to autointeraction for the ith gene.

In order to study a single contact zone, we supply Eq. (1) with the initial condition

$$\psi_i(x, 0) = A_i \theta(\sigma_i(x - X_i(0))) \qquad (4)$$

where $X_i(t)$ is the position of the domain border (activation front), and A_i is the initial concentration. $\sigma_i = \pm 1$ indicates which side of the system is occupied by the ith domain. With $A_i > C_i/\epsilon_{ii}$, these initial conditions ensure the formation of only one activation front per gene. We assume reflective boundary conditions and derive our results in the infinite system, $L \to +\infty$. This is a satisfying approximation to the in-the-bulk dynamics of finite-size systems, as long as $L/2 - |X_i(t)| > \lambda_i$. Limitations are discussed in the Supplemental Material (SM) [63].

A remarkable property of (1) is that $\psi_i(x,t)$ can be found analytically without the prior knowledge of $X_i(t)$. The Green's function of Eq. (1) reads

$$G_i(x - x', t - t') = \frac{e^{-\gamma_i(t-t') - \frac{(x-x')^2}{4D_i(t-t')}}}{\sqrt{4\pi D_i(t - t')}}. \qquad (5)$$

Then, the concentration profile $\psi_i(x,t)$ reads

$$\psi_i(x,t) = \int_{-\infty}^{+\infty} dx'\, G_i(x-x',t)\psi_i(x',0) + \sigma_i H_i \int_0^t dt' \int_{X_i(t')}^{\sigma_i\infty} dx'\, G_i(x-x',t-t'). \quad (6)$$

In order to obtain $X_i(t)$ one must solve the free boundary problem $F_i(\psi_1(X_i(t),t),\psi_2(X_i(t),t)) = 0$ or explicitly

$$\epsilon_{11}\psi_1(X_1(t),t) + \epsilon_{12}\psi_2(X_1(t),t) = C_1$$
$$\epsilon_{21}\psi_1(X_2(t),t) + \epsilon_{22}\psi_2(X_2(t),t) = C_2. \quad (7)$$

By inserting (6) into (7), one finds that $X_1(t)$ and $X_2(t)$ are defined by a system of nonlinear integral equations.

Let us first consider the system without cross-interactions between target genes ($\epsilon_{i\neq j} = 0$), so (7) reduces to $\epsilon_{ii}\psi_i(X_i(t),t) = C_i$. This means that the number of particles at the domain boundary is constant. For $t \gg \gamma_i^{-1}$ we can neglect the influence of initial conditions and multiply this equation by $(\epsilon_{ii}\tilde{\psi}_i)^{-1}$ to obtain

$$\frac{S_i}{2} = \sigma_i\gamma_i \int_0^t dt' \int_{X_i(t')}^{\sigma_i\infty} dx'\, G_i[X_i(t)-x',t-t']. \quad (8)$$

This shows that $X_i(t)$ must evolve in such way that the value of the space-time integral of $G_i[X_i(t)-x',t-t']$ is conserved. This integral represents the number of particles arriving at $X_i(t)$ from the activated region, as G_i is also the transition probability. Graphical analysis, as in Fig. 2(a), shows that this is satisfied for

$$X_i(t) = v_i t + \tilde{X}_i \quad (9)$$

where $\tilde{X}_i$ is a constant. In the SM we also show that $\dot{X}_i(t) = v_i$ is the attractor of dynamics. Similar results were rigorously proven by Terman [64], but our method can be easily extended to the interacting case. The ansatz (9) allows explicit integrations in Eq. (8) (see SM), which, in the limit $t \to +\infty$, leads to the equation

$$S_i = 1 + \sigma_i \frac{v_i}{\sqrt{4D_i\gamma_i + v_i^2}}. \quad (10)$$

In Fig. 2(b) we show v_i calculated from (10) (see SM), which indicates a few different regimes of dynamics. First, let us consider $C_i > 0$, which means the gene is inactive by default. For $0 < S_i < 1$ the expression domain expands with constant velocity, while for $1 < S_i < 2$ it shrinks. For $S_i = 1$ it is long-term stable. $S_i > 2$ and $S_i < 0$ translate into $\epsilon_{ii}\tilde{\psi}_i < C_i$. This means the long-term concentration is too low to sustain activation and an activated domain must collapse in its entire volume over finite time.

For $C_i < 0$, gene is spontaneously expressed everywhere in undifferentiated tissue and traveling fronts do not form, see Fig. 2(c). For $\epsilon_{ii}\tilde{\psi}_i > C_i$, the long-term concentration

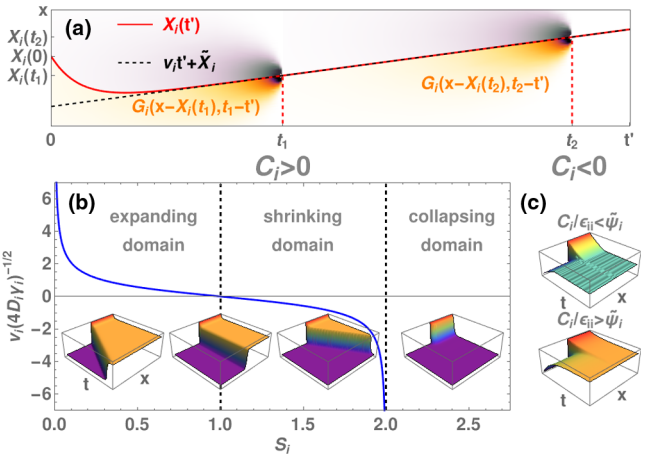

FIG. 2. (a) Illustration of Eq. (8), defining the evolution of domain boundary $X_i(t)$. Density maps in the background show the kernel $G_i[x-X_i(t_i),t-t_i]$ at two moments, t_1 and t_2. Color indicates the space-time area of integration in Eq. (8). The integral of $G_i[x-X_i(t_i),t'-t_i]$ is asymptotically conserved on the line $X_i(t') = v_i t' + \tilde{X}_i$. (b) Single domain dynamics of noninteracting gene for $\sigma_i = -1$ (domain in the region $(-\infty, X_i(t))$), for $C_i > 0$. v_i is calculated from Eq. (10). Insets show corresponding concentration profiles $\psi_i(x,t)$ in different regimes ($S_i = 0.5$, 1.0, 1.5, 2.1, from left to right). (c) Single-gene dynamics for $C_i < 0$ (spontaneous expression). For $C_i/\epsilon_{ii} > \tilde{\psi}_i$ concentration saturates at $\tilde{\psi}_i$ (lower), for $C_i/\epsilon_{ii} < \tilde{\psi}_i$ at C_i/ϵ_{ii} (upper).

tends to $\tilde{\psi}_i$, but for $\epsilon_{ii}\tilde{\psi}_i < C_i$, the system saturates at the highest expression level just before inactivation, which is C_i/ϵ_{ii}. This requires $\epsilon_{ii} < 0$.

Let us now consider the fully interacting case, that is $\epsilon_{ij} \neq 0$ for $i \neq j$. We can repeat the reasoning for the noninteracting case, though this time it is the sum of the autointeraction integral and cross-interaction integral that has to be conserved. The ansatz (9) holds, but with the important change that both velocities must be the same, i.e., $v_1 = v_2 = v$ (see SM). This allows us to turn (7) into the algebraic problem

$$S_i = (1+\sigma_i V_i(v)) + \chi_i[1 + (-1)^i\sigma_j \mathrm{sgn}(\Delta X) + \sigma_j e^{\frac{v\Delta X}{2D_j}((-1)^{i+1}\frac{\mathrm{sgn}(\Delta X)}{V_j(v)})}(V_j(v) - (-1)^i\mathrm{sgn}(\Delta X))] \quad (11)$$

where $V_i(v) = (v/\sqrt{4D_i\gamma_i + v^2})$ and $\Delta X = \tilde{X}_2 - \tilde{X}_1$ is the relative distance between the domain boundaries. We will now discuss the properties of (11) using χ_i (the ratio of cross- to autointeraction strength) as control parameters.

First of all, Eq. (11) indicates the existence of a phase transition between the IGEP and TGEP phases. For clearest presentation, let us consider two autoactivating and cross-inhibiting genes ($\chi_i < 0$), whose expression domains spontaneously expand ($0 < S_i < 1$). The order parameter of transition reads

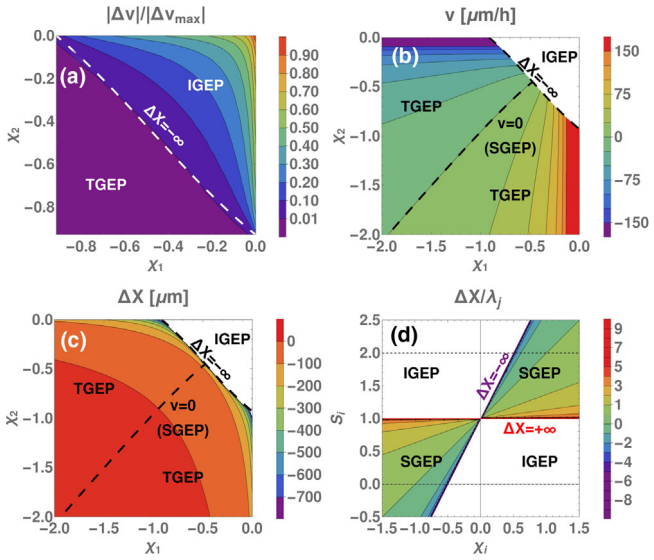

FIG. 3. (a) Map of $|\Delta v|/|\Delta v_{\max}|$ over the (χ_1,χ_2) plane. $\Delta v_{\max}$ is Δv for $(\chi_1,\chi_2)=(0,0)$. Δv is the order parameter of transition between IGEP and TGEP phase. Phase boundary coincides with $\Delta X=-\infty$ line (white, dashed). 3D representation of these data is included in SM. (b),(c) The maps of v and ΔX over the (χ_1,χ_2) plane in TGEP phase. The line $v=0$ indicates SGEPs. (d) The phase diagram of SGEP, in the (χ_i,S_i) space. Colored region indicates where ΔX is defined. Stabilization requires that $\Delta X(\chi_1,S_1)=\Delta X(\chi_2,S_2)$.

$$\Delta v=\lim_{t\to+\infty}[\dot{X}_2(t)-\dot{X}_1(t)] \tag{12}$$

which is the long-term difference of domain wall velocities. Δv dependence on (χ_1,χ_2) is shown in Fig. 3(a). In the IGEP phase $\Delta v\neq 0$, which means that two domains ever-increase their overlap and their boundaries eventually adopt two constant, but different velocities. The $t\to+\infty$ value of ΔX does not exist and Eqs. (11) have no solution. We analytically estimated that the IGEP phase is no smaller than the square $0>\chi_i>(S_i-1)/2$ on the (χ_1,χ_2) plane (see SM). However, simulations show that the boundary of the IGEP phase coincides with the line $\Delta X=-\infty$ on the (χ_1,χ_2) plane.

In the TGEP phase $\Delta v=0$ and Eqs. (11) can be solved for v and ΔX. In this case, upon meeting, the two growing domains establish a contact zone of width ΔX. TGEP domains can still change their size by one expanding and the other shrinking, but the contact zone travels as one entity, preserving ΔX [see Figs. 1(b) and 1(c)]. ΔX and v as the functions of (χ_1,χ_2) are shown in Figs. 3(b) and 3(c). The IGEP-TGEP transition demonstrates that establishing a meaningful GEP requires certain minimal strengths of cross-interactions, below which no patterning is possible. Once the TGEP phase is entered, further increase in interaction strengths drives ΔX from the complete overlap on the critical line ($\Delta X=-\infty$) to the emergence of the gap ($\Delta X\geq 0$).

Finally, SGEPs can be identified as TGEPs with $v=0$. The SGEPs occupy a line on the (χ_1,χ_2) plane [Figs. 3(b) and 3(c)]. In this case Eqs. (11) are overdefined and ensuring that ΔX exists leads to the stability conditions. Let us introduce the auxiliary variable R_i, such that

$$R_i=(S_i-1)/\chi_i-1 \tag{13}$$

then, the stability conditions read

$$\begin{aligned}&(1-|R_1|)^{\lambda_2}=(1-|R_2|)^{\lambda_1},\\&\sigma_1\mathrm{sgn}(R_1)=-\sigma_2\mathrm{sgn}(R_2),\qquad -1\leq R_i\leq 1.\end{aligned} \tag{14}$$

When these dependencies are satisfied, two activated domains form a SGEP with the distance between domain boundaries given by (for $i\neq j$)

$$\Delta X=(-1)^j\sigma_i\mathrm{sgn}(R_j)\lambda_i\ln(1-|R_j|). \tag{15}$$

SGEPs are perfectly stable, i.e., they survive for $t\to+\infty$, but the first of conditions in (14) is restrictive and imposes strong constraints on the parameters. Nevertheless, the SGEP indicates the center of low-velocity plateau in the TGEP phase [see Fig. 3(b)]. The biologically relevant part of this plateau can be estimated to ± 24 μm/h, based on the shift of gap gene domains in *Drosophila* [46,65,66] (see SM).

These stability conditions (14) are valid in the entire range of S_i and χ_i, not only for $0<S_i<1$ and $\chi_i<0$. This allows us to discuss the stability of all 64 two-gene network motifs, described by six constants (four ϵ_{ij} and two C_i), which can be either >0 or <0. We will call a trio $(\epsilon_{ii},\epsilon_{i\neq j},C_i)$ together with node i the "half-motif," as two such trios form a full two-gene motif. There are only eight half-motifs. $(\epsilon_{ii},\epsilon_{i\neq j},C_i)$ can be mapped into the pair of (χ_i,S_i) via Eqs. (3). In stable systems, parameters must be chosen in such a way that point (χ_1,S_1) corresponds to point (χ_2,S_2) with the same ΔX. In Fig. 3(d) we illustrate the SGEP phase diagram of $\Delta X(\chi_i,S_i)$. The phase diagram is symmetric about the point (0,1), so, having (χ_1,S_1) fixed, (χ_2,S_2) can be chosen in two ways. In order to classify the stability of the resulting pattern it is enough to check to which part of phase diagram in Fig. 3(d) each of the half-motifs constituting the full network motif can be assigned. SGEPs are formed only from the two potentially stable half-motifs.

In Fig. 4 the stability regions of all possible half-motifs are shown. For half-motifs with $C_i>0$, stabilization is the result of competition between interactions and the spontaneous behavior of domains. For $(+,+,+)$ and $(-,+,+)$ activation is counterbalanced by the spontaneous shrinking or collapsing of domains ($S_i>1$ and $S_i<0$, respectively). For these cases, the boundaries of initial domains must be placed within λ_i's range, so the stabilization precedes their

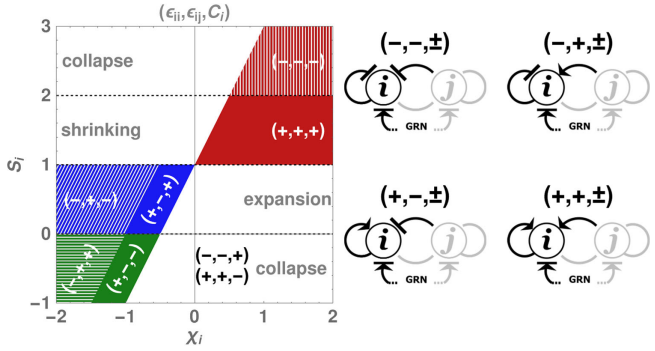

FIG. 4. Half-motifs $(\epsilon_{ii}, \epsilon_{i\neq j}, C_i)$ and their stability regions. Colored fields indicate the stability of self-activating half-motifs ($\epsilon_{ii} > 0$), which overlap with the stability regions of self-repressive half-motifs ($\epsilon_{ii} < 0$, dashed fields).

spontaneous decay. The half-motif $(+,-,+)$ is less restrictive for initial conditions, as it involves a spontaneously growing domain ($0 < S_i < 1$). Combinations of $(+,-,+)$ with $(-,+,+)$ are often encountered in biological systems, such as spinal cord development [43], limb formation [26,51–53], and segmentation in the *Drosophila* embryo [46,47].

For half-motifs with $C_i < 0$ stabilization is the result of competition between the default activation ($C_i < 0$) and inhibiting interactions. There are no restrictions for initial conditions, as genes with $C_i < 0$ are spontaneously expressed in undifferentiated tissue.

Two half-motifs cannot be stabilized: $(-,-,+)$ and $(+,+,-)$. The former has no activating interactions, thus it cannot sustain expression in the long run. Conversely, the latter is activated by default and by both interactions, thus it spreads in an unbounded manner. Interestingly, half-motif $(-,-,C_i)$ is found in many biological systems [39,43,46,47], but our results show that it requires external activation ($C_i < 0$) to ensure stability.

Finally, the stability of half-motifs with $\epsilon_{ii} < 0$ has an additional limitation. In the two-gene system, the effective threshold for activation reads $\tilde{C}_i = C_i - \epsilon_{ij}\psi_j$. Similar to one-component systems, when $\tilde{C}_i < 0$ and $\epsilon_{ii}\tilde{\psi}_i < \tilde{C}_i$, the production of the ith gene tends to $\tilde{C}_i/\epsilon_{ii}$ instead of $\tilde{\psi}_i$. This causes the stability conditions to fail when $S_i < 2 + 2\chi_i$ for $(-,+,\pm)$ and when $S_i < 2$ for $(-,-,-)$.

We have shown that the quasinonlinear model provides an in-depth insight into the problem of GEP stabilization. It elucidates the single-gene dynamics and demonstrates that the formation of biologically relevant GEPs (traveling or genuinely stable) is governed by a phase transition. Further, it provides stability conditions for two-gene network motifs encountered in developmental GRNs. Our predictions should hold for systems with additional genes and interactions, as long as contact zones between domains are separated by at least λ_i, which allows us to consider them separately. The model also exhibits much potential for further generalizations.

We thank T. Sokolowski and B. Waclaw for comments on the manuscript. The research for this publication has been supported by a grant from the Priority Research Area DigiWorld under the Strategic Programme Excellence Initiative at Jagiellonian University. M. M. and M. Z. were supported by the Polish National Agency for Academic Exchange. R. H. and M. Z. were supported by the Narodowe Centrum Nauki, Poland (SONATA, 2017/26/D/NZ2/00454).

*maciej.majka@uj.edu.pl
†Present address: The Njord Centre, Department of Physics, University of Oslo, P.O. Box 1048 Blindern, 0316 Oslo, Norway.
‡marcin.zagorski@uj.edu.pl

[1] J. Norbury and A. M. Stuart, IMA J. Appl. Math. **39**, 241 (1987).
[2] H. P. McKean and V. Moll, Bull. Am. Math. Soc. **12**, 255 (1985).
[3] I. Idris and V. N. Biktashev, Phys. Rev. Lett. **101**, 244101 (2008).
[4] G. Arioli and H. Koch, Nonlinear Anal. Theory **113**, 51 (2015).
[5] G. R. North, J. Atmos. Sci. **32**, 2033 (1975).
[6] S. Bensid and J. I. Díaz, arXiv:1808.03979.
[7] P. A. Stephens, W. J. Sutherland, and R. P. Freckleton, Oikos **87**, 185 (1999).
[8] E. Brunet and B. Derrida, Phys. Rev. E **56**, 2597 (1997).
[9] D. A. Kessler, Z. Ner, and L. M. Sander, Phys. Rev. E **58**, 107 (1998).
[10] R. J. Allen and B. Waclaw, Rep. Prog. Phys. **82**, 016601 (2018).
[11] G. Q. Sun, Nonlinear Dyn. **85**, 1 (2016).
[12] B. A. Grzybowski, K. J. Bishop, C. J. Campbell, M. Fialkowski, and S. K. Smoukov, Soft Matter **1**, 114 (2005).
[13] A. Arango-Restrepo, D. Barragán, and J. M. Rubi, Phys. Chem. Chem. Phys. **21**, 17475 (2019).
[14] T. Bollenbach, K. Kruse, P. Pantazis, M. González-Gaitán, and F. Jülicher, Phys. Rev. Lett. **94**, 018103 (2005).
[15] A. Kicheva, P. Pantazis, T. Bollenbach, Y. Kalaidzidis, T. Bittig, F. Jülicher, and M. González-Gaitán, Science **315**, 521 (2007).
[16] T. Gregor, E. F. Wieschaus, A. P. McGregor, W. Bialek, and D. W. Tank, Cell **130**, 141 (2007).
[17] S. Y. Shvartsman and R. E. Baker, Wiley Interdiscip. Rev. Dev. Biol. **1**, 715 (2012).
[18] P. Müller, K. W. Rogers, S. R. Yu, M. Brand, and A. F. Schier, Development **140**, 1621 (2013).
[19] K. S. Stapornwongkul and J. P. Vincent, Nat. Rev. Genet. **22**, 393 (2021).
[20] P. McHale, W.-J. Rappel, and H. Levine, Phys. Biol. **3**, 107 (2006).
[21] D. Ben-Zvi, B.-Z. Shilo, A. Fainsod, and N. Barkai, Nature (London) **453**, 1205 (2008).

[22] D. Ben-Zvi and N. Barkai, Proc. Natl. Acad. Sci. U.S.A. **107**, 6924 (2010).
[23] D. M. Umulis and H. G. Othmer, Development **140**, 4830 (2013).
[24] A. Kicheva and J. Briscoe, Trends Cell Biol. **25**, 579 (2015).
[25] D. Aguilar-Hidalgo, S. Werner, O. Wartlick, M. González-Gaitán, B. M. Friedrich, and F. Jülicher, Phys. Rev. Lett. **120**, 198102 (2018).
[26] R. Mateus, L. Holtzer, C. Seum, Z. Hadjivasiliou, M. Dubois, F. Jülicher, and M. González-Gaitán, Cell Rep. **30**, 4292 (2020).
[27] M. Zagorski, Y. Tabata, N. Brandenberg, M. P. Lutolf, G. Tkačik, T. Bollenbach, J. Briscoe, and A. Kicheva, Science **356**, 1379 (2017).
[28] M. D. Petkova, G. Tkačik, W. Bialek, E. F. Wieschaus, and T. Gregor, Cell **176**, 844 (2019).
[29] K. Exelby, E. Herrera-Delgado, L. G. Perez, R. Perez-Carrasco, A. Sagner, V. Metzis, P. Sollich, and J. Briscoe, Development **148**, dev197566 (2021).
[30] J. Jaeger, S. Surkova, M. Blagov, H. Janssens, D. Kosman, K. N. Kozlov, Manu, E. Myasnikova, C. E. Vanario-Alonso, M. Samsonova, D. H. Sharp, and J. Reinitz, Nature (London) **430**, 368 (2004).
[31] Y. Morishita and Y. Iwasa, Biophys. J. **101**, 2324 (2011).
[32] K. ichi Hironaka and Y. Morishita, Curr. Opin. Genet. Dev. **22**, 553 (2012).
[33] T. R. Sokolowski, T. Erdmann, and P. R. ten Wolde, PLoS Comput. Biol. **8**, e1002654 (2012).
[34] H. Tran, J. Desponds, C. Angelica, P. Romero, C. Fradin, N. Dostatni, and A. M. Walczak, PLoS Comput. Biol. **14**, e1006513 (2018).
[35] J. Jaeger and B. Verd, *Dynamic Positional Information: Patterning Mechanism versus Precision in Gradient-Driven Systems*, 1st ed. (Elsevier Inc., New York, 2020), Vol. 137.
[36] G. Tkačik and T. Gregor, Development **148**, dev176065 (2021).
[37] N. M. Luscombe, M. M. Babu, H. Yu, M. Snyder, S. a Teichmann, and M. Gerstein, Nature (London) **431**, 308 (2004).
[38] G. T. Reeves, C. B. Muratov, T. Schüpbach, and S. Y. Shvartsman, Dev. Cell **11**, 289 (2006).
[39] U. Alon, Nat. Rev. Genet. **8**, 450 (2007).
[40] J. Cotterell and J. Sharpe, Mol. Syst. Biol. **6**, 425 (2010).
[41] Z. Burda, A. Krzywicki, O. C. Martin, and M. Zagorski, Proc. Natl. Acad. Sci. U.S.A. **108**, 17263 (2011).
[42] A. D. Lander, Cell **144**, 955 (2011).
[43] N. Balaskas, A. Ribeiro, J. Panovska, E. Dessaud, N. Sasai, K. M. Page, J. Briscoe, and V. Ribes, Cell **148**, 273 (2012).
[44] O. C. Martin, A. Krzywicki, and M. Zagorski, Phys. Life Rev. **17**, 124 (2016).
[45] A. Jiménez, J. Cotterell, A. Munteanu, and J. Sharpe, Mol. Syst. Biol. **13**, 925 (2017).
[46] B. Verd, A. Crombach, and J. Jaeger, PLoS Comput. Biol. **13**, e1005285 (2017).
[47] B. Verd, N. A. M. Monk, and J. Jaeger, eLife **8**, e42832 (2019).
[48] V. Ribes, N. Balaskas, N. Sasai, C. Cruz, E. Dessaud, J. Cayuso, S. Tozer, L. L. Yang, B. Novitch, E. Marti, and J. Briscoe, Genes Dev. **24**, 1186 (2010).
[49] K. Kuzmicz-Kowalska and A. Kicheva, WIREs Dev. Biol. Publ. **10**, e383 (2020).
[50] T. Shinozuka and S. Takada, J. Dev. Biol. **9**, 30 (2021).
[51] J. Raspopovic, L. Marcon, L. Russo, and J. Sharpe, Science **345**, 566 (2014).
[52] L. Marcon, X. Diego, J. Sharpe, and P. Müller, eLife **5**, e14022 (2016).
[53] A. N. Landge, B. M. Jordan, X. Diego, and P. Müller, Dev. Biol. **460**, 2 (2020).
[54] R. Vuilleumier, A. Springhorn, L. Patterson, S. Koidl, M. Hammerschmidt, M. Affolter, and G. Pyrowolakis, Nat. Cell Biol. **12**, 611 (2010).
[55] O. Wartlick, P. Mumcu, A. Kicheva, T. Bittig, C. Seum, F. Jülicher, and M. González-Gaitán, Science **331**, 1154 (2011).
[56] O. Wartlick, F. Jülicher, and M. González-Gaitán, Development **141**, 1884 (2014).
[57] W. A. Alaynick, T. M. Jessell, and S. L. Pfaff, Cell **146**, 178 (2011).
[58] A. Kicheva, T. Bollenbach, A. Ribeiro, H. P. Valle, R. Lovell-Badge, V. Episkopou, and J. Briscoe, Science **345**, 1254927 (2014).
[59] S. Vakulenko, Manu, J. Reinitz, and O. Radulescu, Phys. Rev. Lett. **103**, 168102 (2009).
[60] S. Rulands, B. Klünder, and E. Frey, Phys. Rev. Lett. **110**, 038102 (2013).
[61] T. Gregor, D. W. Tank, E. F. Wieschaus, and W. Bialek, Cell **130**, 153 (2007).
[62] T. R. Sokolowski and G. Tkačik, Phys. Rev. E **91**, 062710 (2015).
[63] See Supplemental Material at http://link.aps.org/supplemental/10.1103/PhysRevLett.130.098402 for detailed derivation of analytical results, additional information on figures and estimation of biologically relevant parameter range.
[64] D. Terman, SIAM J. Math. Anal. **14**, 1107 (1983).
[65] T. A. Markow, S. Beall, and L. M. Matzkin, J. Evol. Biol. **22**, 430 (2009).
[66] J. Jaeger, M. Blagov, D. Kosman, K. N. Kozlov, Manu, E. Myasnikova, S. Surkova, C. E. Vanario-Alonso, M. Samsonova, D. H. Sharp, and J. Reinitz, Genetics **167**, 1721 (2004).